Search for the Higgs boson in the di-photon decay channel with ATLAS detector

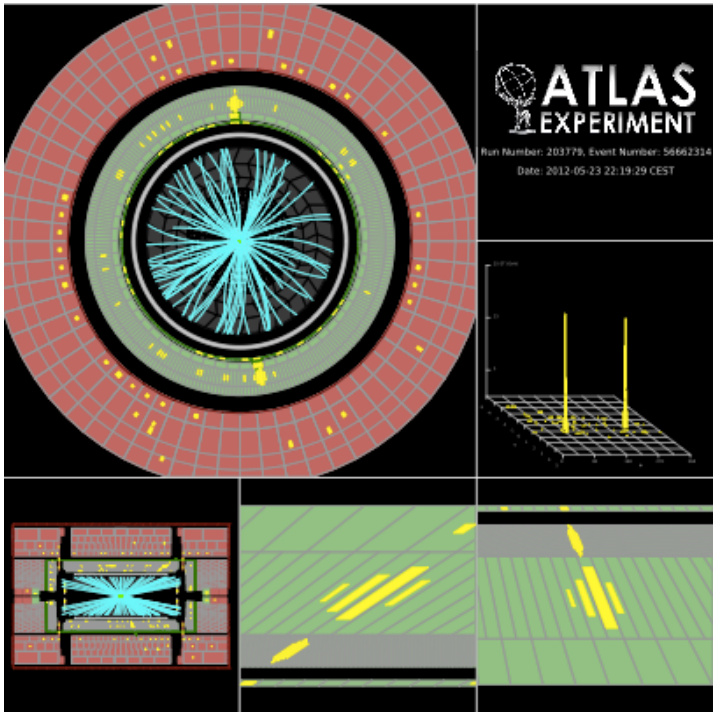

Marcos Jimenez (DESY)
On Behalf of the ATLAS Collaboration
Hadron Collider Physics, Kyoto Nov. 14th 2012

SM Higgs → γγ Searches

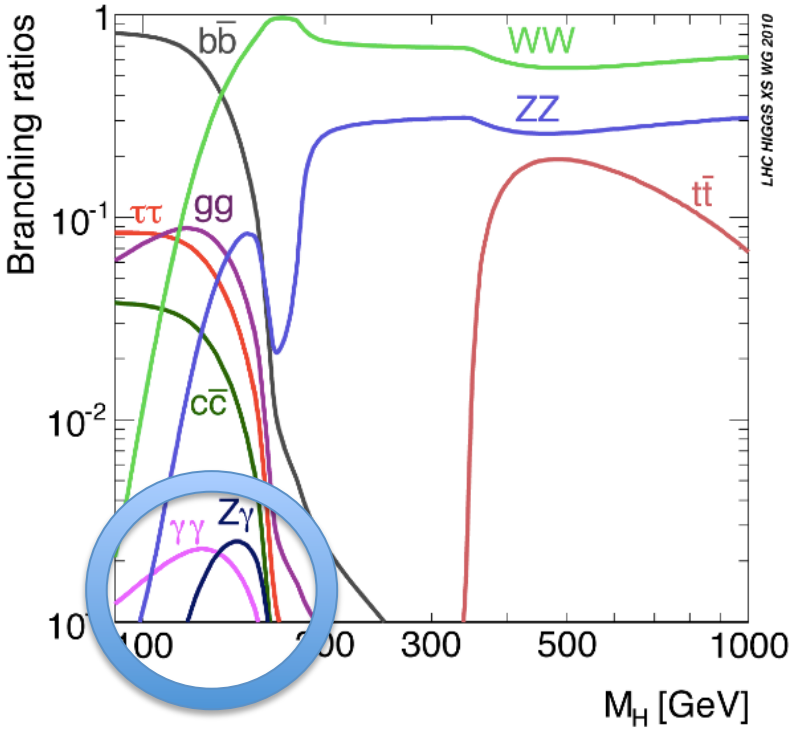

Crucial ingredients $m_{\gamma\gamma}^2 = 2 * E_1 E_2 (1 - \cos \alpha)$

- ❑ **Robust photon reco, isolation and identification**
- ❑ **Good energy calibration and primary vertex reconstruction (*α depends on PV and cluster position*)**
- ❑ **Good background modeling**

- ➢ ***Relative low branching fraction expected from the SM***
- ➢ ***Relatively high (but reducible) backgrounds : π^0 -jets faking photons***

However, "simple" analysis and event signature:

- ❑ **Two high pT photons :**
  $pT_1 > 40$ GeV and $pT_2 > 30$ GeV
  (di-photon trigger efficiency ~99%)
- ❑ **Tight photon criteria to reject background (shower cuts and isolation):**
  event selection efficiency ~40%

> ➢ Signal expected as **narrow resonance over smooth decaying background**

- ❑ **Split data-sample into categories to best exploit detector response and expected S/B :** range from 3-10 %

In this presentation

- Dataset :
  - → 4.9 fb^{-1} with 7 TeV data
  - → 5.9 fb^{-1} with 8 TeV data

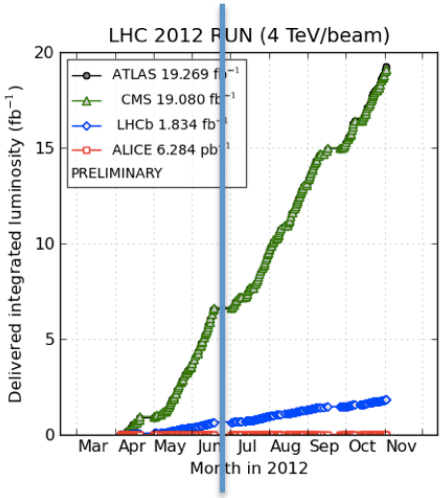

- **Analysis done separately for 7 and 8 TeV and combined statistically**
- **Ambitious campaign underway** to include a larger data-set

OUTINE

I. Photon reconstruction
II. Photon Isolation
III. Photon Identification
IV. Primary vertex
V. Energy Calibration
VI. Background modeling

VII. Categories

VIII. Limits/signal strength

IX. Resonance properties
(see Haijun's talk!)

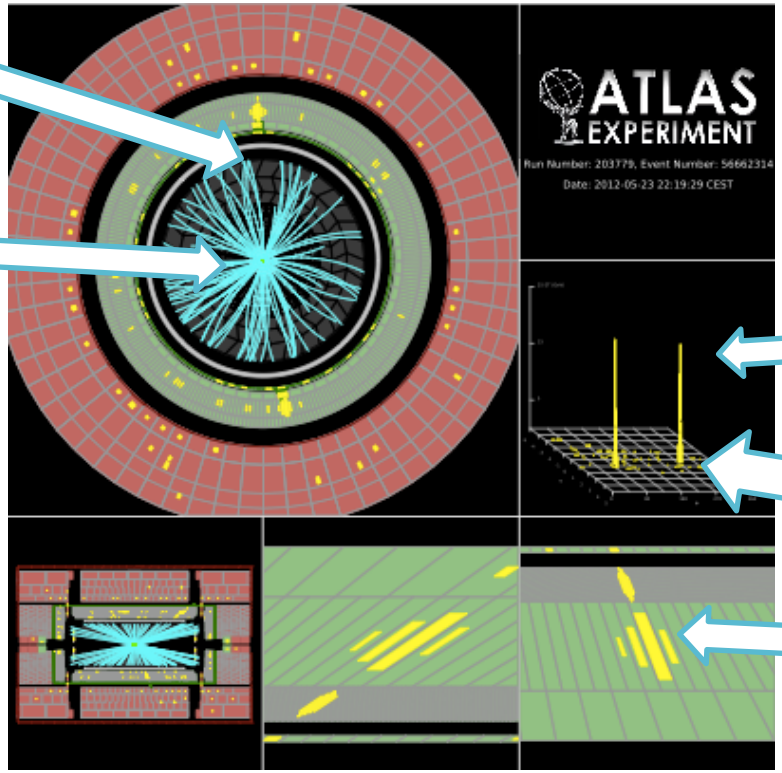

Energy Calibration

Photon Isolation

Photon Identification

Photon ID 1 – Photon reconstruction and isolation

- **Photon reconstruction from clusters in LAr calorimeter and conversion vertices in Inner Detector → must be robust against (challenging) pileup conditons**

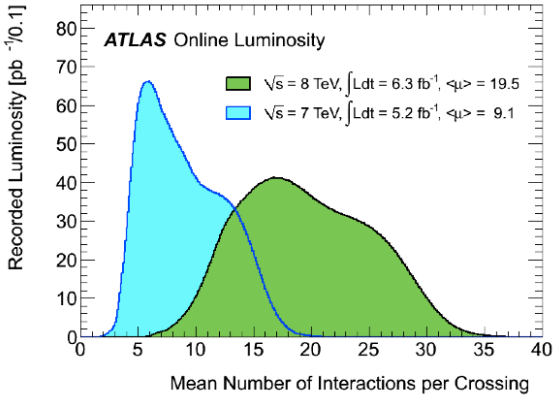

- Fraction of conv/unconv photons as a function of the <number> of interactions per bunch crossing stable

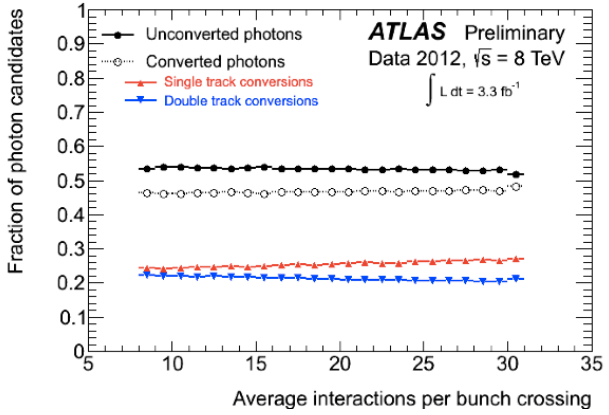

- **ISOLATION → from positive-energy topological clusters in calorimeter with ΔR < 0.4**

Cell-based isolation (old)

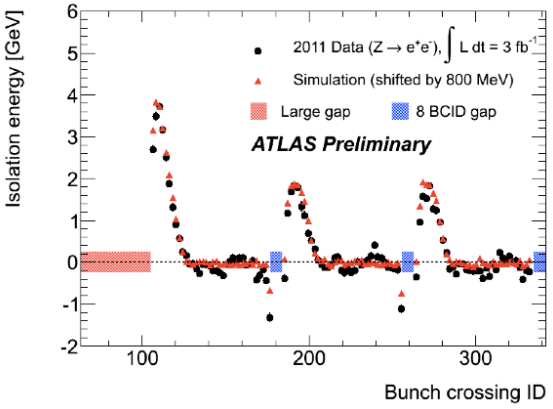

Cluster-based isolation (new)

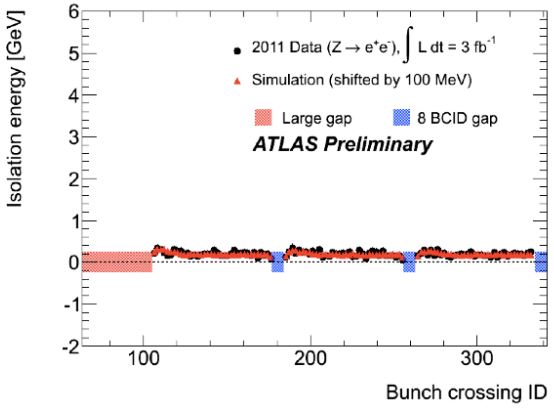

- Good stability with position of colliding bunches in train → **robust with pileup**
- Better MC/data agreement
- Better resolution

Photon ID 2 – Photon shower shapes and background rejection

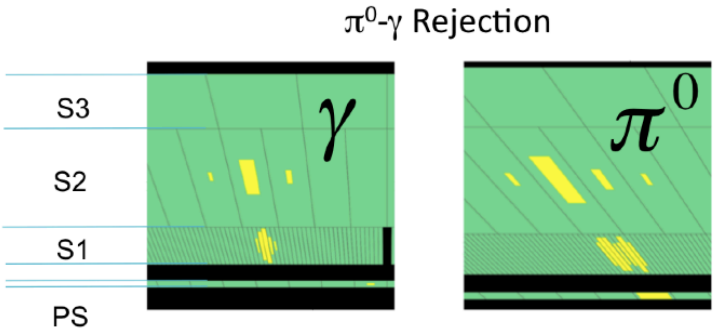

➢ **Photons shower shape distributions in LAr sampling layers - different for signal and background (π^0)**

- ❑ For 7 TeV data Neural Net is deployed to identify photons based on shower shapes
- ❑ For 8 TeV data cut-based approach is used

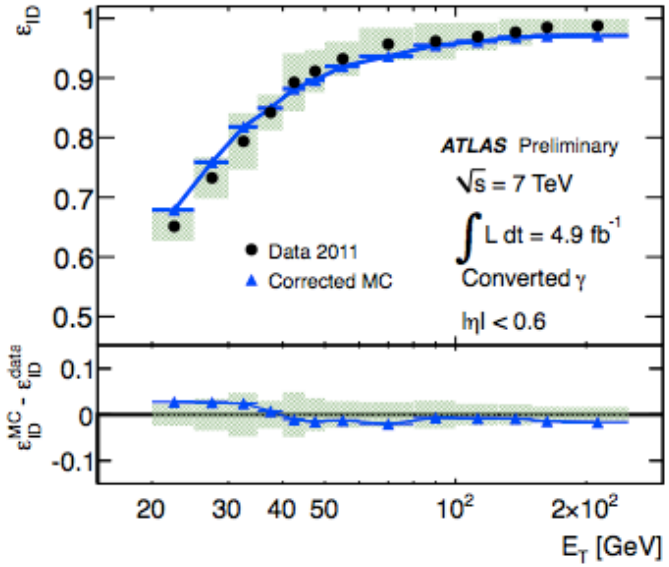

➢ **Data-driven methods used to determine photon identification efficiency and estimate uncertainty of MC prediction**

→ Photon ID uncertainty < 5% above 40 GeV (dominant uncertainty ~10% on signal yield)

→ Uncertainty in photon ID treated as fully correlated between different photon eta regions

Background Composition

- In order to gain understanding of the SM background, several data-driven methods are deployed to estimate the different background components
- **Methods are based on measuring background properties (isolation template, pass/fail shower criteria) in a background enriched region and extrapolating to the signal region**

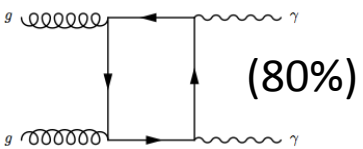

(80%)

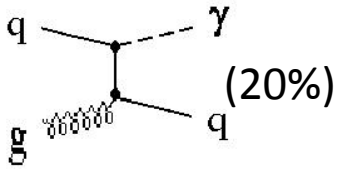

(20%)

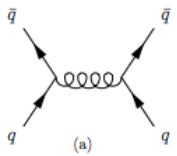

(1%)

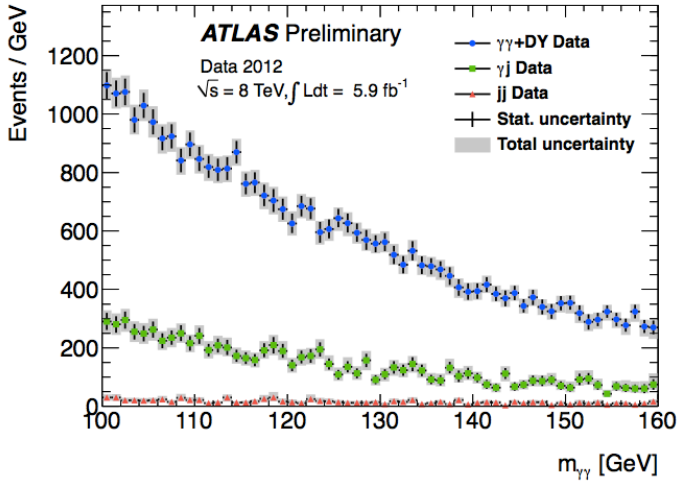

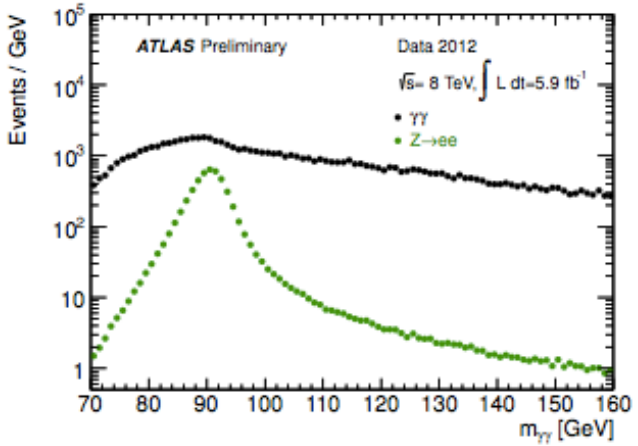

- Consistent background composition (di-photon purity of ~80%, γj ~20%, jj~1-2%)
  → used to assess best photon ID working point (in terms of expected S/B)
- In addition, the electron contamination is also estimated to be << 1%

Vertex Reconstruction

$$m_{\gamma\gamma}^2 = 2 E_1 E_2 (1 - \cos\alpha)$$

- Important for position measurement of photons and for determining if jets come from hard interaction or from pileup (VBF category in next slides)
- Vertex reconstructed through likelihood combination

- Calorimeter 'pointing'
- Σ tracks pT^2
- Conversion vertex
- Mean vertex position

Calo pointing

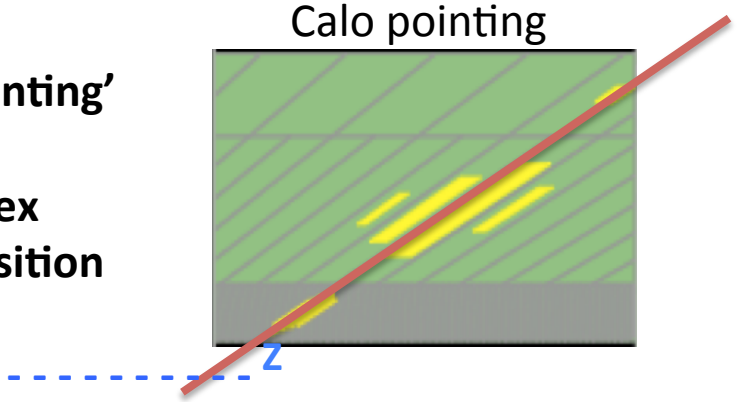

Method vs $M_{\gamma\gamma}$ resolution

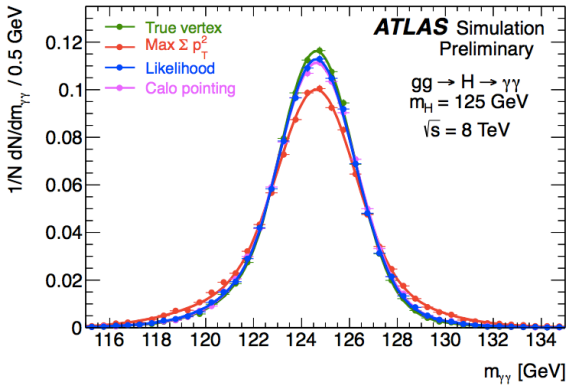

Pileup vs $M_{\gamma\gamma}$ resolution

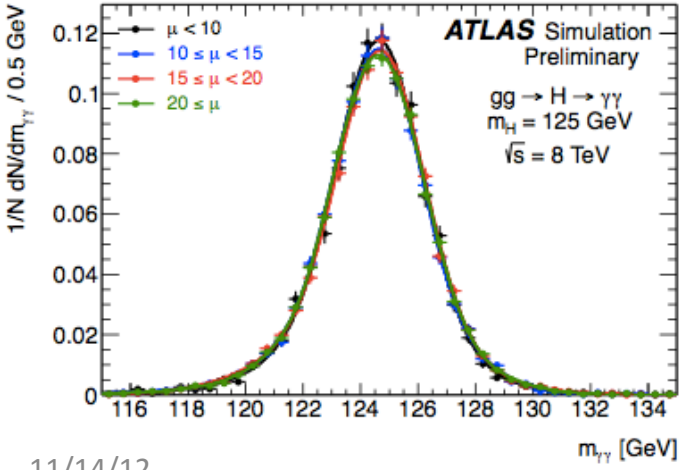

Efficiency vs pileup

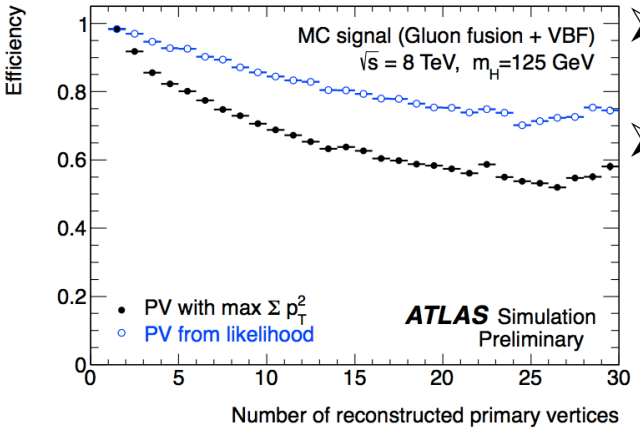

- Important for VBF category
- Jet criteria : with respect to PV

Energy Calibration and resolution

$$m_{\gamma\gamma}^2 = 2 * E_1 E_2 (1 - \cos\alpha)$$

- MC based calibration corrects measured cluster energy by loss due to (longitudinal/transverse) leakage, dead material in front of EMC and sampling energy loss (MC-based)
- Energy scale and residual mis-modeling of MC-based calibration corrected for by in-situ Z→ee data/MC comparison (cross checked with J/ψ, W→eν) – extrapolated to photons (cross-checked with radiative Z sample)
- Energy scale at m_Z known to 0.3%, uniformity (constant term) 1% in barrel, 1.2 – 2.1% in endcap

Agreement between data & MC Z→ee lineshape

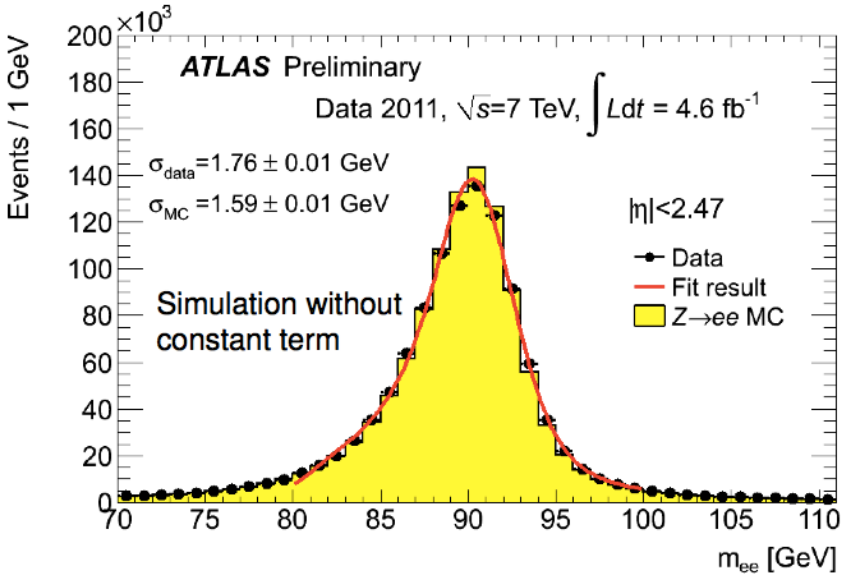

Expected resolution of Higgs signal (best vs worst category)

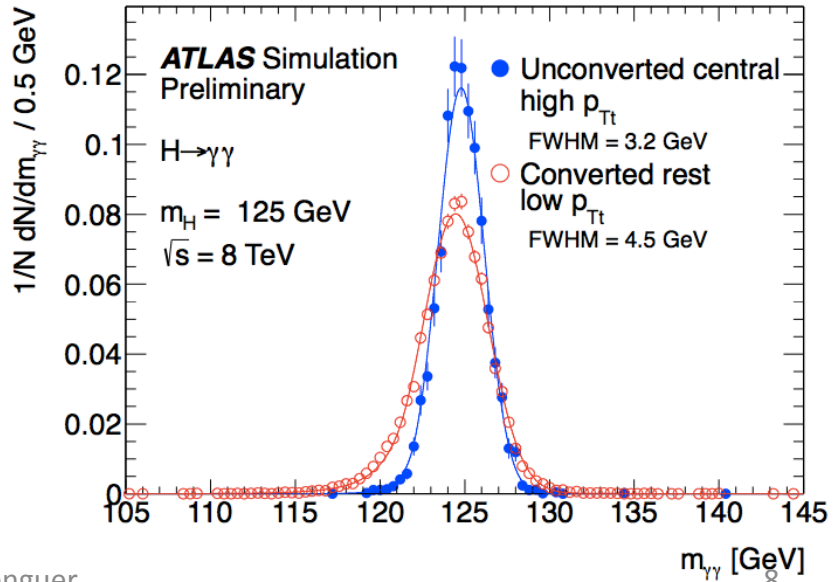

Event categorization

Event categories based on eta, pTt, and conversion, (2-jet category – next slide!)

Both unconverted:

- Central
- Rest

At least one converted:

- Central
- Transition
- Rest

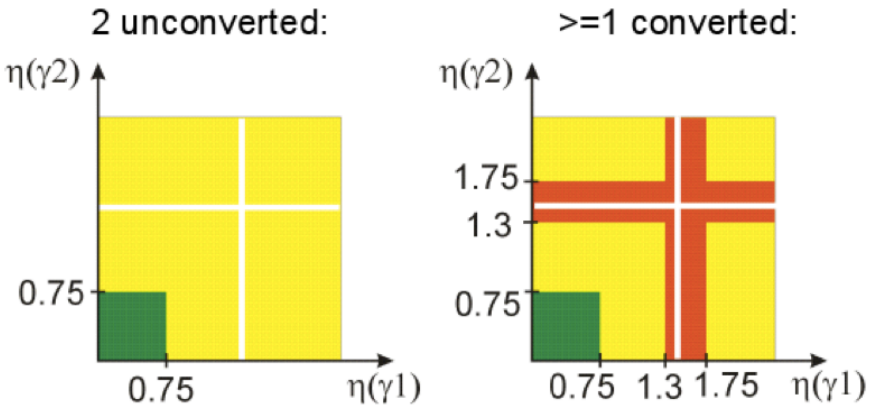

Resolution:

Good
Medium
Poor

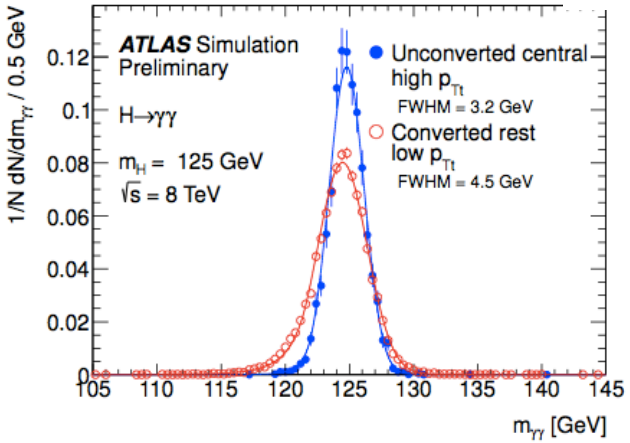

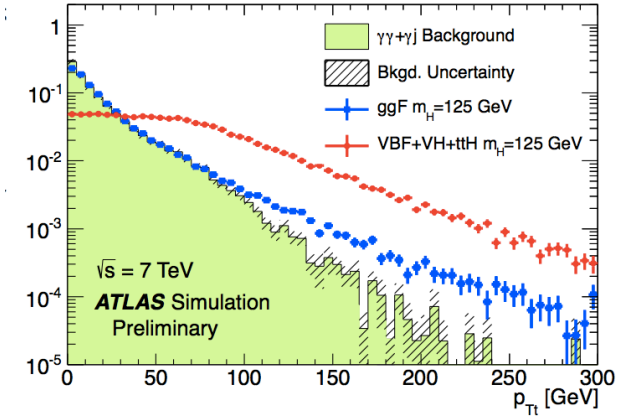

Central and Rest divided into $p_{Tt} < 60$ GeV and $p_{Tt} > 60$ GeV

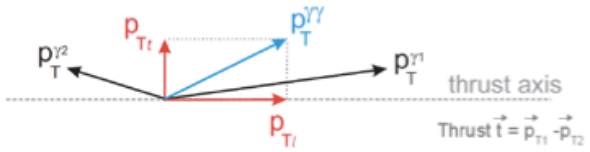

- Categorization exploits different S/B (3-10%), detector response (resolution) and statistics

VBF-enriched category

- Separate events consistent with VBF signature to enhance sensitivity to Higgs production in VBF

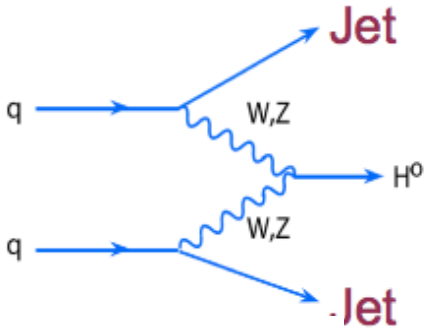

Signature

- Two high pT jets from the PV and Δϕγγ-jj > 2.6
- Separated in rapidity: Δηjj > 2.8 and mjj > 400 GeV

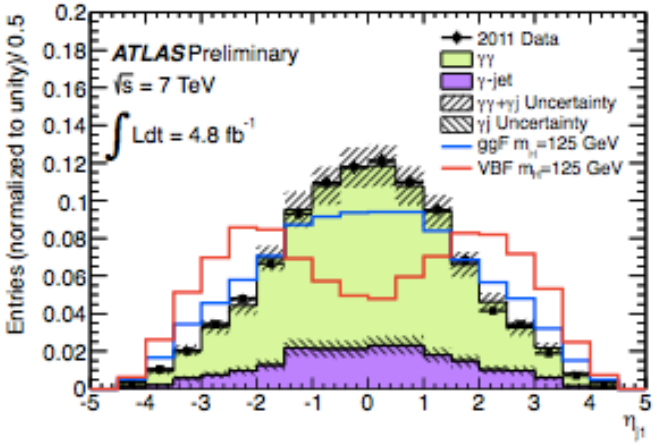

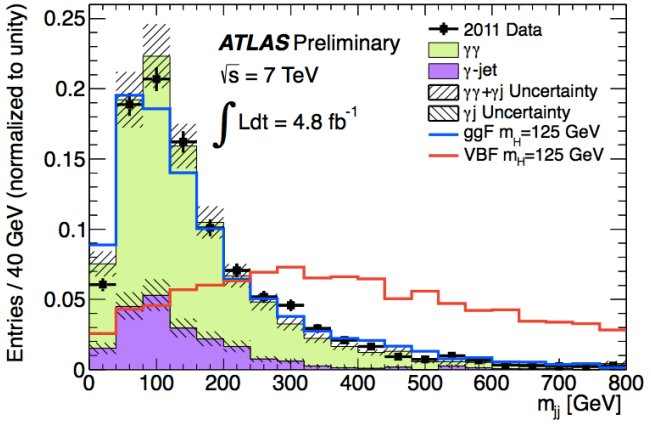

- **Expected VBF selection efficiency for each production process (for 2012 but similar for 2011)**

$\sqrt{s}$ Category	Events	$gg \to H$ [%]	VBF [%]	WH [%]	ZH [%]	ttH [%]
2-jets	2.9	30.4	68.4	0.4	0.2	0.2

- Large uncertainty on gluon-fusion contamination due to that on the perturbative calculation (25%) and UE model (30%)

Signal and Background model (experimental)

- Signal is modeled using a **crystal ball** function (width dominated by detector resolution) **+ broad gaussian** to account for poorly reconstructed energy

- **Functional form of background is determined using MC but normalization and parameters set using fit to data $M_{\gamma\gamma}$ distribution**

Background models are tested for possible bias

- **Accept model if the spurious signal is < 10% of expected signal or < 20% of fitted signal uncertainty ("spurious" defined by fitting S+B model to B only MC)**
- Among the models left, choose the one with the best expected p_0 at 125 GeV

Category	Parametrization	Uncertainty [N_{evt}]	
		$\sqrt{s}$ = 7 TeV	$\sqrt{s}$ = 8 TeV
Inclusive	4th order pol.	7.3	10.6
Unconverted central, low p_{Tt}	Exp. of 2nd order pol.	2.1	3.0
Unconverted central, high p_{Tt}	Exponential	0.2	0.3
Unconverted rest, low p_{Tt}	4th order pol.	2.2	3.3
Unconverted rest, high p_{Tt}	Exponential	0.5	0.8
Converted central, low p_{Tt}	Exp. of 2nd order pol.	1.6	2.3
Converted central, high p_{Tt}	Exponential	0.3	0.4
Converted rest, low p_{Tt}	4th order pol.	4.6	6.8
Converted rest, high p_{Tt}	Exponential	0.5	0.7
Converted transition	Exp. of 2nd order pol.	3.2	4.6
2-jets	Exponential	0.4	0.6

- **Low statistics categories tend to be modeled by simple exponentials** whereas more complex **polynomials are used for high statistics categories**
- **For theory cross/ section, BF etc.. (arXiv: 1207.7214)**

Signal and Background model (categories)

→ Only some examples here. In total 10 categories (in 2011 and 2012, respectiv.)

Unconverted central, low pT t (8 TeV)

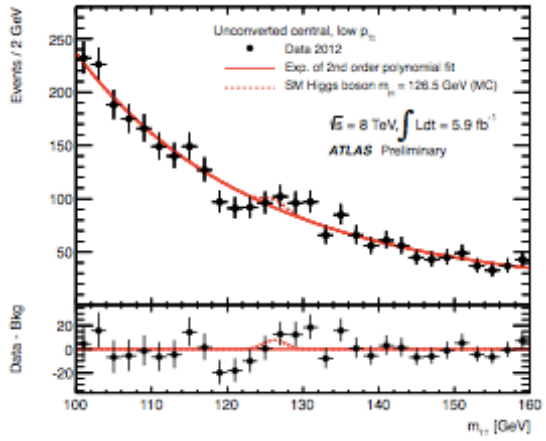

Converted central, low pT t (7 TeV)

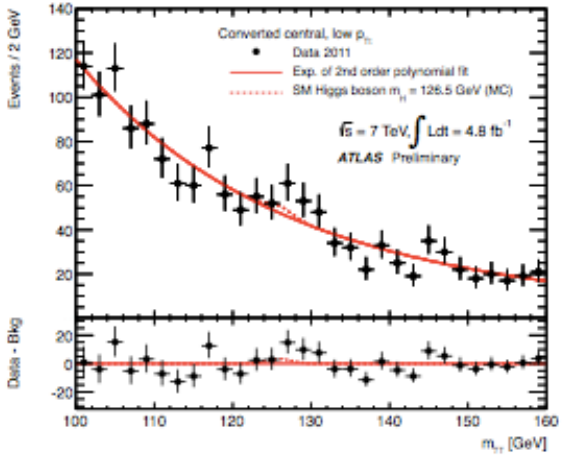

2jet (8 TeV)

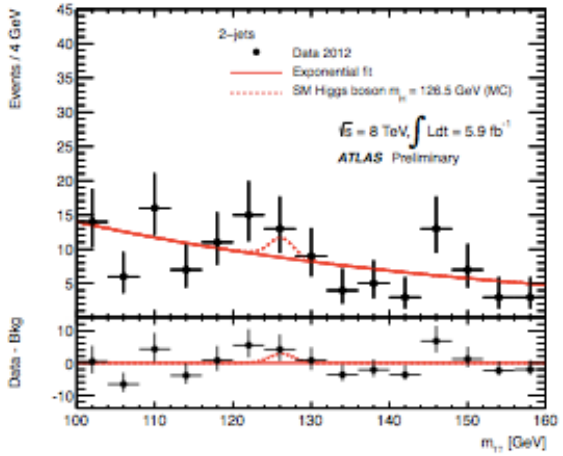

Converted rest, high pT t (7 TeV)

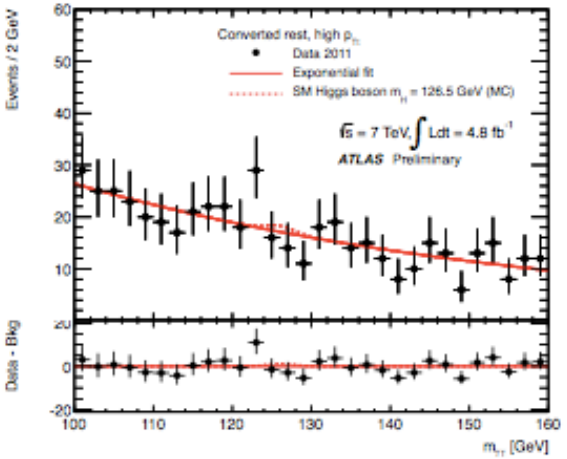

Invariant Mass distribution

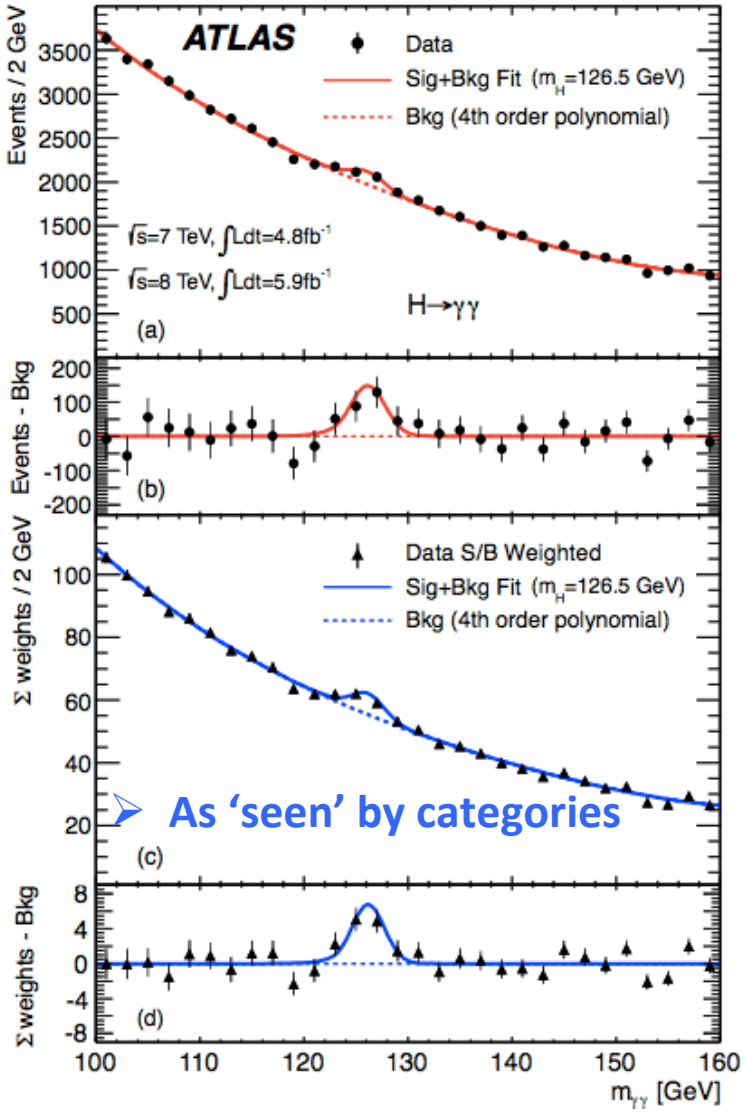

➢ As 'seen' by categories

Dominant sources of systematic uncertainty on yield

- ❑ Photon ID efficiency ~10%
- ❑ Energy resolution ~14% and mass scale ~0.6%
- ❑ Isolation < 1%
- ❑ Pileup 4%
- ❑ Lumi 1-3.6 % (2011-2012)
- ❑ Theory cross section
  - ~ up to 25% (for VBF contribution)
  - ~ up to 12% (in other ggF)

  (underlying event ~5% and PTt dist up to 12% at hight PTt)

- ❑ Bkg Param (evts) 0.2-4.6 (0.3-6.8) for 2011(2012)

In VBF category

- ❑ Jet E-scale 9-10%
- ❑ Underl. Evt. 6-30%
- ❑ Higgs p_T up to 12.5%

23788 events (7 TeV) and 35251 events (8 TeV)

Background+signal fit, signal fixed at 126.5 GeV

Signal Strength

- SM hHggs excluded in the regions of **112 – 122.5 GeV and 132 – 143 GeV**
- Best fitted signal strength (wrt SM) for $m_{\gamma\gamma}$ = 126 of **$\mu = 1.8 \pm 0.5$**

→ **signal strength is the overall factor by which the SM Higgs production cross sections are scaled to get the best fit to the excess observed in data**

- CL limit on σ/σ_{SM}

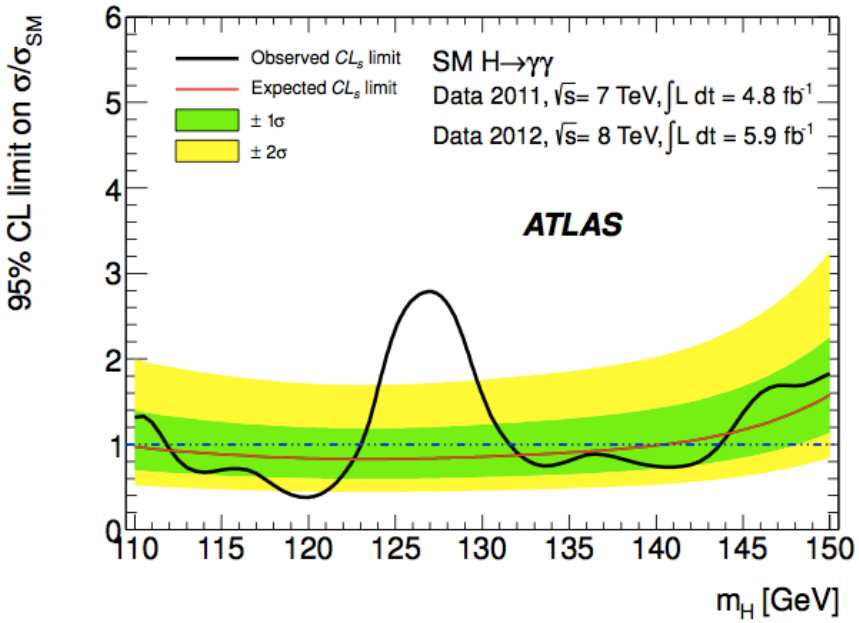

Signal Strength per Category

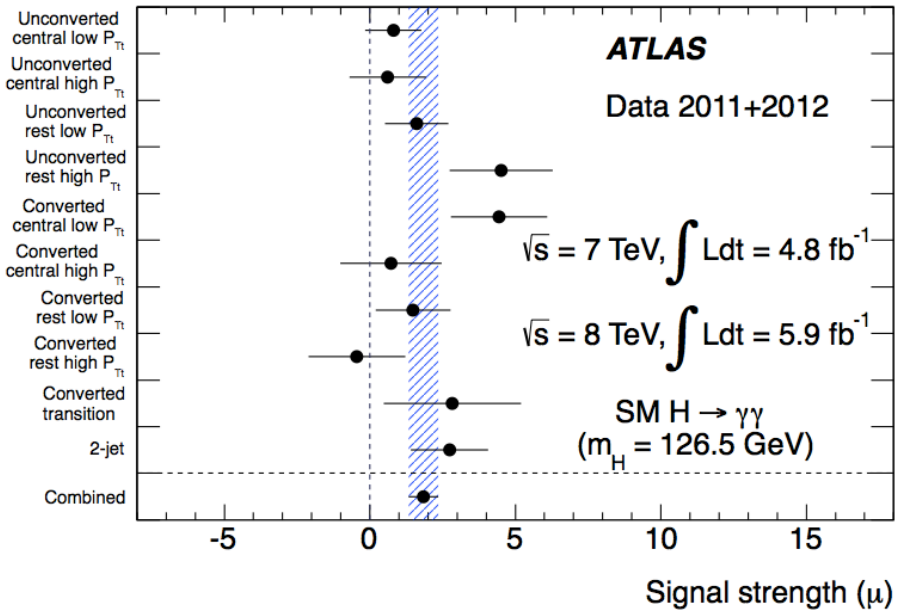

Quantifying the excess

- **Maximum deviation from background only expectation at $m_{\gamma\gamma}$ 126.5 GeV**

→ **Local significance 4.5σ** ***(expected from SM Higgs 2.4σ)***

Effect of combination of 2011 & 2012

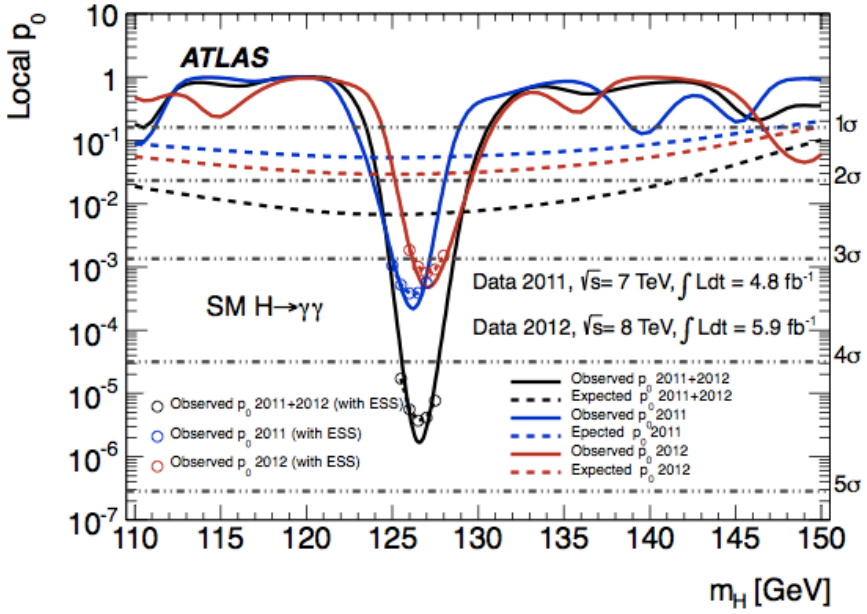

Effect of adding VBF category

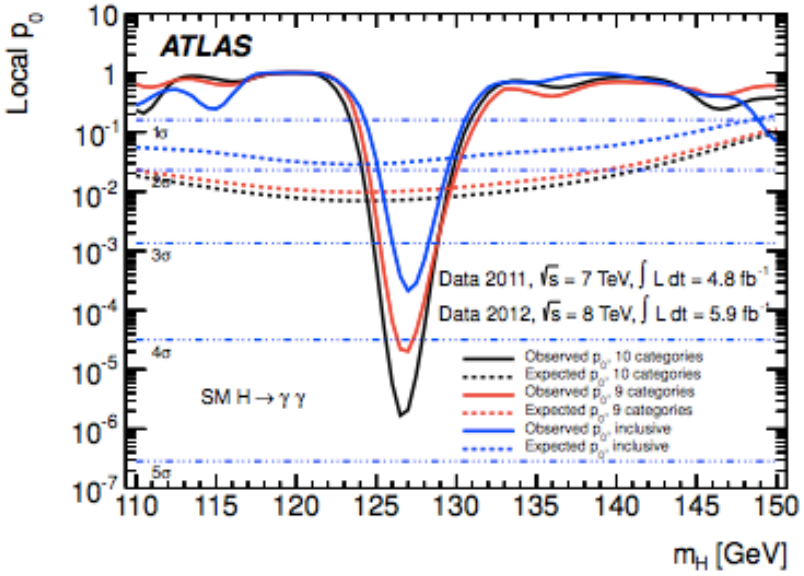

- ***Results consistent between 2011 and 2012 and improved by VBF category***
- ***Results consistent between inclusive analysis (no categories) and with categories***

Properties of new resonance

- **Mass**

  → **Likelihood contours in the (μ, mH) plane. Uncertainty on fit comparable for statistical and systematic uncertainty**

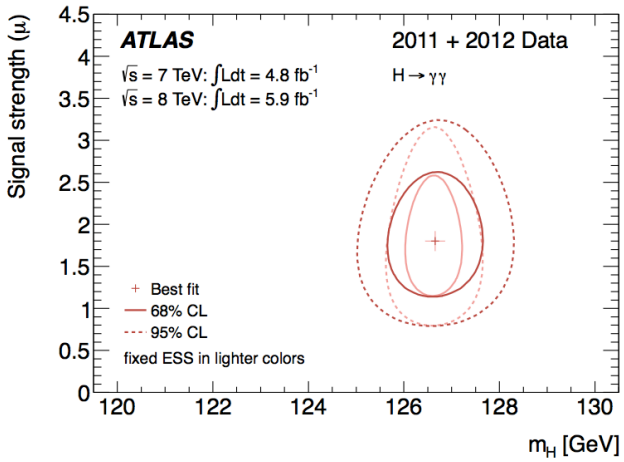

- **With and without ES uncertainty**

- **Couplings**

  → **Constraints in the plane of μ (ggF+*tt̄H* ×B/B_{SM}) and μ (VBF+*VH* × B/B_{SM}), where *B* is the branching ratio for *H*→γγ, can be obtained**

  → **The data are compatible with the SM at the 1.5 σ level**

- **Production modes merged due to similar couplings and small stats (with current data-set)**

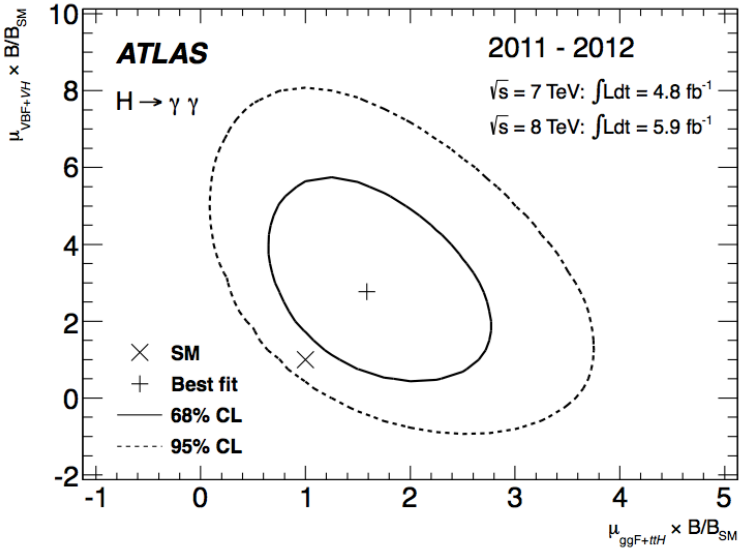

Summary and conclusions

- **Observation of a narrow excess in the diphoton mass spectrum around 126.5 GeV with a local significance of 4.5σ (global 3.6σ)**
- **Signal strength with respect to SM prediction, μ = 1.8±0.5**
- **Agreement with SM prediction within 2 sigma**

- Results well documented:
  - → **ATLAS-CONF-2012-091**
  - → arXiv:1207.7214
  - → **ATLAS-CONF-2012-127**

- **Kappa factors. Combination of H→γγ, H→ZZ, H→WW, H→ττ, H→bb channels (ATLAS-CONF-2012-127)**

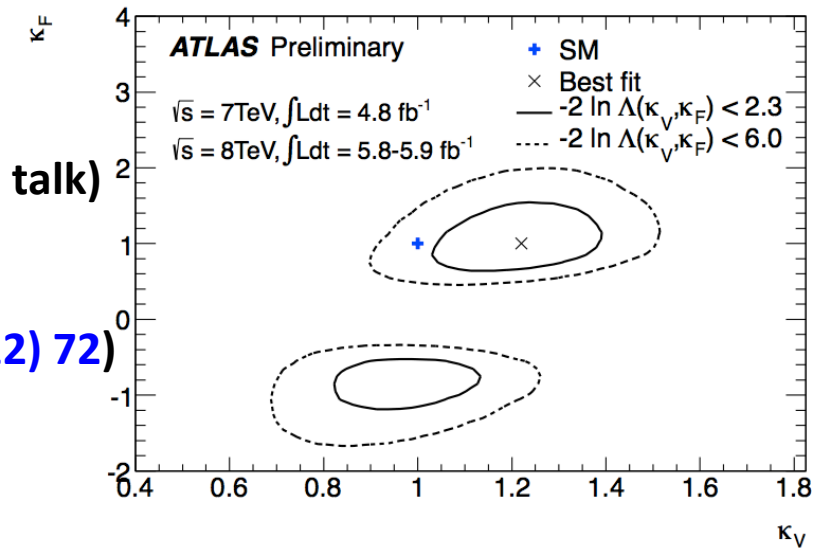

- **Combination with other channels (Haijun's talk)**

- **Extensions of H→γγ analysis carried out**
  - → **fermiophobic model (Eur. Phys. J. C (2012) 72)**
  - → **cp-odd scalar (ATLAS-CONF-2012-079)**

- **Next steps (with enlarged data-set):**
  - Establish the true nature of excess with property measurements
  - **Mass, Spin/CP, relative strengths (define VH and ttH categories)**

BACK-UP

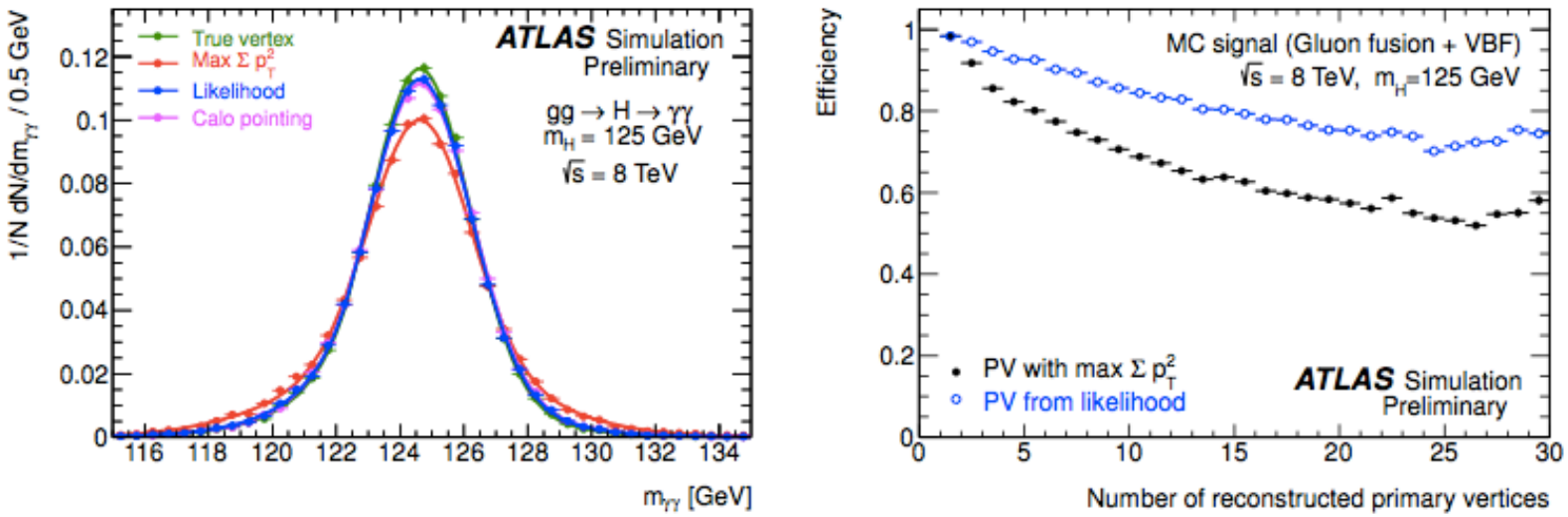

Figure 1: Left: distribution of the expected diphoton mass for $H \rightarrow \gamma\gamma$ signal events as a function of the algorithm used to determine the longitudinal vertex position of the hard-scattering event. The use of the calorimeter information, labelled as "Calo pointing" is fully adequate to reach the optimal achievable mass resolution labelled as "True vertex". The likelihood described in the text, combining this information with the primary vertex information from the tracking, provides similar mass resolution. Right: the dependence of the efficiency for selecting a reconstructed primary vertex within $\Delta z = 0.2$ mm of the true hard interaction vertex using two different methods: the highest $\sum p_{\mathrm{T}}^2$ of all tracks assigned to a vertex (black) and from the likelihood as described in the text (blue). The addition of the tracking information from the inner detector is necessary to improve the efficiency of identification of the hard-interaction primary vertex needed for the jet selection.

BACK-UP

Table 6: Number of expected signal events per category at $m_H = 126.5$ GeV, at $\sqrt{s} = 7$ TeV (top) and $\sqrt{s} = 8$ TeV (bottom) and breakdown by production process.

$\sqrt{s}$	Category	Events	$gg \to H$ [%]	VBF [%]	WH [%]	ZH [%]	ttH [%]
7 TeV	Inclusive	79.3	87.8	7.3	2.9	1.6	0.4
	Unconverted central, low p_{Tt}	10.4	92.9	4.0	1.8	1.0	0.2
	Unconverted central, high p_{Tt}	1.5	66.5	15.7	9.9	5.7	2.4
	Unconverted rest, low p_{Tt}	21.6	92.8	3.9	2	1.1	0.2
	Unconverted rest, high p_{Tt}	2.7	65.4	16.1	10.8	6.1	1.8
	Converted central, low p_{Tt}	6.7	92.8	4.0	1.9	1.0	0.2
	Converted central, high p_{Tt}	1.0	66.6	15.3	10	5.7	2.5
	Converted rest, low p_{Tt}	21.0	92.8	3.8	2.0	1.1	0.2
	Converted rest, high p_{Tt}	2.7	65.3	16.0	11.0	5.9	1.8
	Converted transition	9.5	89.4	5.2	3.3	1.7	0.3
	2-jets	2.2	22.5	76.7	0.4	0.2	0.1
8 TeV	Inclusive	111.6	88.5	7.4	2.7	1.6	0.5
	Unconverted central, low p_{Tt}	14.4	92.9	4.2	1.7	1.0	0.2
	Unconverted central, high p_{Tt}	2.5	72.5	14.1	6.9	4.2	2.3
	Unconverted rest, low p_{Tt}	31.4	92.5	4.1	2.0	1.1	0.2
	Unconverted rest, high p_{Tt}	5.3	72.1	13.8	7.8	4.6	1.7
	Converted central, low p_{Tt}	9.1	92.8	4.3	1.7	1.0	0.3
	Converted central, high p_{Tt}	1.6	72.7	13.7	7.1	4.1	2.3
	Converted rest, low p_{Tt}	27.3	92.5	4.2	2.0	1.1	0.2
	Converted rest, high p_{Tt}	4.6	70.8	14.4	8.3	4.7	1.7
	Converted transition	13.0	88.8	6.0	3.1	1.8	0.4
	2-jets	2.9	30.4	68.4	0.4	0.2	0.2

BACK-UP

Table 2: Number of expected signal S and background events B in mass a window around m_H = 126.5 GeV that would contain 90% of the expected signal events, along with the observed number of events in this window. In addition, σ_{CB}, the Gaussian width of the Crystal Ball function describing the invariant mass distribution (see Sec. 6), and the FWHM of the distribution, are given. The numbers are given for the data and simulation at $\sqrt{s}$ = 8 TeV for different categories and the inclusive sample.

Category	σ_{CB} [GeV]	FWHM [GeV]	Observed [N_{evt}]	S [N_{evt}]	B [N_{evt}]
Inclusive	1.63	3.87	3693	100.4	3635
Unconverted central, low p_{Tt}	1.45	3.42	235	13.0	215
Unconverted central, high p_{Tt}	1.37	3.23	15	2.3	14
Unconverted rest, low p_{Tt}	1.57	3.72	1131	28.3	1133
Unconverted rest, high p_{Tt}	1.51	3.55	75	4.8	68
Converted central, low p_{Tt}	1.67	3.94	208	8.2	193
Converted central, high p_{Tt}	1.50	3.54	13	1.5	10
Converted rest, low p_{Tt}	1.93	4.54	1350	24.6	1346
Converted rest, high p_{Tt}	1.68	3.96	69	4.1	72
Converted transition	2.65	6.24	880	11.7	845
2-jets	1.57	3.70	18	2.6	12

BACK-UP

Table 5: Expected Higgs boson signal efficiency ϵ (including acceptance of kinematic selections as well as photon identification and isolation efficiencies) and event yield for $H \to \gamma\gamma$ assuming an integrated luminosity of 4.8 fb^{-1} for the $\sqrt{s} = 7$ TeV data (top) and of 5.9 fb^{-1} for the $\sqrt{s} = 8$ TeV data (bottom). Results are given for different production processes.

$\sqrt{s}$	m_H [GeV]	$gg \to H$		VBF		WH		ZH		ttH		Total
		ϵ(%)	N_{evt}	ϵ(%)	N_{evt}	ϵ(%)	N_{evt}	ϵ(%)	N_{evt}	ϵ(%)	N_{evt}	N_{evt}
7 TeV	110	37.3	71.7	37.9	5.2	33.5	2.8	33.5	1.5	33.7	0.4	81.6
	115	39.5	73.8	40.1	5.5	34.9	2.8	35.5	1.5	34.9	0.3	83.9
	120	40.9	73.5	42.1	5.8	37.0	2.6	36.9	1.4	35.9	0.3	83.6
	125	42.0	70.9	43.8	5.8	38.1	2.4	38.4	1.3	37.2	0.3	80.7
	130	43.1	66.3	44.8	5.7	39.3	2.1	39.9	1.2	37.8	0.3	75.6
	135	44.6	59.8	46.9	5.3	40.7	1.8	40.8	1.0	38.7	0.2	68.1
	140	45.2	51.7	48.7	4.8	41.8	1.5	42.3	0.9	39.5	0.2	59.1
	145	45.8	42.3	49.8	4.1	42.5	1.2	43.6	0.7	40.5	0.2	48.5
	150	45.8	31.6	49.7	3.1	44.1	0.9	44.7	0.5	40.7	0.1	36.2
8 TeV	110	33.8	100.6	34.5	7.4	29.9	3.7	29.5	2.1	27.3	0.6	114.4
	115	35.6	103.8	36.2	7.9	30.6	3.6	32.5	2.1	27.9	0.6	118.0
	120	37.2	103.6	38.1	8.2	32.7	3.4	32.9	2.0	29.4	0.6	117.8
	125	38.3	100.3	39.6	8.3	33.9	3.2	34.2	1.8	29.7	0.5	114.1
	130	39.1	94.1	41.2	8.0	35.1	2.8	35.9	1.6	31.1	0.5	107.0
	135	40.4	85.3	42.4	7.6	35.7	2.4	36.6	1.4	32.2	0.4	97.1
	140	41.1	74.0	43.0	6.8	37.0	2.0	36.8	1.2	32.4	0.3	84.3
	145	41.6	60.6	43.7	5.8	38.0	1.6	38.5	0.9	33.6	0.3	69.2
	150	41.7	45.3	44.8	4.4	38.2	1.1	39.2	0.7	34.0	0.2	51.7

BACK-UP

Table 7: Summary of systematic uncertainties on the expected signal and the background. The values given are the relative uncertainties on these quantities from the various sources investigated for a Higgs boson mass of 125 GeV, except for the case of background modeling, where the uncertainties are provided in Table 3 in terms of the number of events. The sign in the front of values for each systematic uncertainty shows correlations among categories and processes.

Systematic uncertainties	$\sqrt{s}$ = 7 TeV [%]	$\sqrt{s}$ = 8 TeV [%]
Signal event yield		
Photon identification	±8.4	±10.8
Effect of pileup on photon rec/ID	±4	
Photon energy scale	±0.3	
Photon Isolation	±0.4	±0.5
Trigger	±1	
Higgs boson cross section (perturbative)	$gg \to H$: $^{+12}_{-8}$, VBF: ±0.3, WH: $^{+0.2}_{-0.8}$, ZH: $^{+1.4}_{-1.6}$, ttH: $^{+3}_{-9}$	$gg \to H$: $^{+7}_{-8}$, VBF: ±0.2, WH: $^{+0.2}_{-0.6}$, ZH: $^{+1.6}_{-1.5}$, ttH: $^{+4}_{-9}$
	$gg \to H$ + 2 jets: ±25	
Higgs boson cross section (PDF+α_S)	$gg \to H$: $^{+8}_{-7}$, VBF: $^{+2.5}_{-2.1}$, VH: ±3.5, ttH: ±9	$gg \to H$: $^{+8}_{-7}$, VBF: $^{+2.6}_{-2.8}$, VH: ±3.5, ttH: ±8
Higgs boson branching ratio	±5	
Higgs boson p_T modeling	low p_{Tt}: ±1.1, high p_{Tt}: ∓12.5, 2-jets: ∓9	
Underlying Event (2-jets)	VBF: ±6, Others: ±30	
Luminosity	±1.8	±3.6
Signal category migration		
Material	Unconv: ±4, Conv: ∓3.5	
Effect of pileup on photon rec/ID	Unconv: ±3, Conv: ∓2, 2-jets: ±2	Unconv: ±2, Conv: ∓2, 2-jets: ±12
Jet energy scale	low p_{Tt}	
	$gg \to H$: ±0.1, VBF: ±2.6, Others: ±0.1	$gg \to H$: ±0.1, VBF: ±2.3, Others: ±0.1
	high p_{Tt}	
	$gg \to H$: ±0.1, VBF: ±4, Others: ±0.1	$gg \to H$: ±0.1, VBF: ±4, Others: ±0.1
	2-jets	
	$gg \to H$: ∓19, VBF: ∓8, Others: ∓15	$gg \to H$: ∓18, VBF: ∓9, Others: ∓13
Jet-vertex-fraction		2-jets: ±13, Others: ∓0.3
Primary vertex selection	negligible	
Signal mass resolution		
Calorimeter energy resolution	±12	
Electron to photon extrapolation	±6	
Effect of pileup on energy resolution	±4	
Primary vertex selection	negligible	
Signal mass position		
Photon energy scale	±0.6	
Background modeling	see Table 3	